DOI: 10.1002/ejic.200701065

Comparison of Isoelectronic Heterometallic and Homometallic Binuclear Cyclopentadienylmetal Carbonyls: The Iron–Nickel vs. the Dicobalt Systems

Jun D. Zhang,[a] Zhongfang Chen,[a][‡] R. Bruce King,*[a] and Henry F. Schaefer, III*[a]

Keywords: Iron / Nickel / Cyclopentadienyl complexes / Carbonyl ligands / Density functional theory

The heterometallic binuclear cyclopentadienylironnickel carbonyl compounds $Cp_2FeNi(CO)_n$ (n = 3, 2, 1; Cp = η^5-C_5H_5) have been studied by density functional theory (BP86) for comparison with the isoelectronic homometallic dicobalt derivatives $Cp_2Co_2(CO)_n$. The FeNi tricarbonyl is shown to be the doubly bridged isomer $Cp_2Fe(CO)Ni(\mu\text{-}CO)_2$ with an Fe–Ni distance of 2.455 Å (BP86), in accord with experiment and in contrast to $Cp_2Co_2(CO)_3$ where singly and triply bridged but not doubly bridged isomers are found. The dicarbonyl compounds $Cp_2FeNi(\mu\text{-}CO)_2$ and $Cp_2Co_2(\mu\text{-}CO)_2$ both have analogous doubly bridged structures with M=M distances around 2.35 Å, suggesting formal M=M double bonds. The monocarbonyl compounds have analogous singly bridged axial structures $Cp_2FeNi(\mu\text{-}CO)$ and $Cp_2Co_2(\mu\text{-}CO)$ with metal–metal distances in the range 2.05 Å (M_2 = Co_2) to 2.12 Å (M_2 = FeNi) consistent with the formal M≡M triple bonds required for the favored 18-electron configuration. Open-shell states of $Cp_2FeNi(\mu\text{-}CO)$ are found to have even lower energies than the closed-shell structure, which indicates that the ground state of $Cp_2FeNi(\mu\text{-}CO)$ might be a high spin structure. However, the global minimum for the monocarbonyl is found to be a singlet "hot dog" perpendicular $Cp_2NiFe(CO)$ structure with a terminal CO group bonded to the iron atom. Other higher energy perpendicular structures are also found for $Cp_2FeNi(CO)_n$ (n = 3, 2, 1) with terminal CO groups and bridging Cp rings.

1. Introduction

A variety of unsaturated homonuclear cyclopentadienylmetal carbonyl compounds have been prepared since the original report[1] of $(\eta^5\text{-}Me_5C_5)_2Mo_2(CO)_4$ in 1967, including $Cp_2V_2(CO)_5$,[2] $Cp_2M_2(CO)_4$ (M = Cr,[3] Mo[4]), and $Cp_2M'_2(CO)_3$ (M′ = Mn,[5] Re[6]) with formal M≡M triple bonds and $Cp_2Re_2(CO)_4$,[7] $Cp_2Fe_2(CO)_3$,[8] and $Cp_2M''_2(CO)_2$ (M″ = Co,[9] Rh[10]) with formal M=M double bonds (Cp = η^5-C_5H_5 or substitution product thereof). In addition, a variety of heteronuclear cyclopentadienylmetal carbonyl compounds are known with heteronuclear metal–metal single bonds.[11] However, no unsaturated heteronuclear cyclopentadienylmetal carbonyls have been prepared containing formal heteronuclear metal–metal multiple bonds. A possible explanation, which has yet to be explored, is that these unsaturated transition metal complexes may prefer ground state structures with open-shell high spin metal atoms rather than closed-shell structures with formal metal–metal multiple bonds.

This paper describes the use of density functional theory (DFT) to investigate possible binuclear cyclopentadienylmetal carbonyl derivatives containing either multiple iron–nickel bonds or open-shell iron–nickel pairs. The iron–nickel system was chosen for this initial study for the following reasons: (1) The "saturated" derivative $Cp_2FeNi(CO)_3$ has been known since 1960[12,13] as well as its phosphane substitution products of the type $(\eta^5\text{-}C_5H_5)_2FeNi(CO)_2L$ [L = PPh_3, PPh_2CH_2, $PPh(CH_3)_2$, $P(CH_3)_3$ and $P(OPh)_3$];[14,15] (2) The isoelectronic dicobalt derivatives are well-characterized experimentally with the isolation and structural characterization of both $Cp_2Co_2(CO)_3$[16] and $Cp_2Co_2(CO)_2$,[9] with formal Co–Co single and Co = Co double bonds, respectively, as well as theoretically using DFT methods.[17] Furthermore, $Cp_2Co_2(CO)$, with a formal Co≡Co triple bond, is a probable intermediate in the formation of its dimer, namely $Cp_4Co_4(\mu_3\text{-}CO)_2$, in the pyrolysis of $Cp_3Co_3(CO)_3$.[18] We focus on the competition between high-spin structures and multiple metal–metal bonds in the formation of "unsaturated" $Cp_2FeNi(CO)$ and the isoelectronic $Cp_2Co_2(CO)$.

2. Theoretical Methods

DFT is a powerful tool in computational transition-metal chemistry,[19] since it provides reliable and useful predictions for the structures and electronic properties of naked transition metal dimers,[20] trimers,[21] and organometallic compounds.[22–30] Extensive experience suggests that the pure GGA functional BP86 is often more reliable for

[a] Department of Chemistry and Center for Computational Chemistry, University of Georgia, Athens, Georgia 30602, USA
[‡] Current address: Department of Physics, Applied Physics and Astronomy, Rensselaer Polytechnic Institute, Troy, New York 12180-3590, USA
Supporting information for this article is available on the WWW under http://www.eurjic.org or from the author.

many organometallic systems than the popular hybrid functional B3LYP when compared with available experimental results.[17,31,32,33] In the present study, complete geometrical optimization and vibrational frequency analyses were carried out using the DFT functional BP86 with DZP basis sets. The BP86 functional combines Becke's 1988 exchange functional (B) with Perdew's 1986 correlation functional.[34,35] Both restricted and unrestricted DFT methods were used to explore the singlet and high spin ground states, respectively. Computational results using the B3LYP functional with a DZP basis set are presented as Supporting Information for comparison.

In this work, the DZP basis set used for carbon and oxygen adds one set of pure spherical harmonic d functions with orbital exponents $\alpha_d(C) = 0.75$ and $\alpha_d(O) = 0.85$ to the Huzinaga–Dunning standard contracted DZ sets[36,37] and is designated as (9s5p1d/4s2p1d). For H, a set of p polarization functions, $\alpha_p(H) = 0.75$, is added to the set to give H(4s1p/2s1p). For Fe and Ni, a loosely contracted DZP basis set, the Wachters primitive set[38] augmented by two sets of p functions and a set of d functions, contracted following Hood, Pitzer and Schaefer,[39] and designated as (14s11p6d/10s8p3d), was used.

Geometrical optimizations and vibrational frequency analyses were performed at the same level of theory discussed above. The second derivatives of the system energy with respect to the nuclear coordinates were evaluated analytically to determine vibrational frequencies. The corresponding infrared intensities were also evaluated analytically. All of the computations were carried out with the Gaussian 94 and Gaussian 03 programs,[40] in which the Ultrafine grid consisting of 99 radical shells with 590 angular points per shell was chosen for evaluating integrals numerically in order to eliminate low magnitude imaginary frequencies caused by numerical error.[41] Both closed-shell singlet and open-shell triplet electronic states were investigated for each $Cp_2FeNi(CO)_n$ structure (n = 3, 2, 1). The lowest quintet state was also investigated for the $Cp_2FeNi(CO)$ structures.

In the search for minima, low magnitude imaginary vibrational frequencies are suspicious, because the numerical integration procedures used in existing DFT methods have significant limitations.[41] Thus, an imaginary vibrational frequency of magnitude less than 10 $i$cm^{-1} should imply that there is a minimum with energy identical to or close to that of the stationary point in question. In most cases we do not follow the eigenvectors corresponding to imaginary vibrational frequencies less than 10 $i$cm^{-1} in search of another minimum.[42]

3. Results and Discussion

In general the molecular structures of singlet and higher spin electronic states of $Cp_2FeNi(CO)_n$ isomers are found for each formula to have related geometrical frameworks using the BP86 method. Information on the optimized structures (Figure 1, Figure 2, Figure 3, and Figure 4) is reported in Table 1, Table 2, and Table 3 accordingly. The listed information includes the dihedral angle $\tau_{(H1–C2–C3–H4)}$ indicating the relative orientation of the two cyclopentadienyl rings. For example, a dihedral angle of 0° indicates an eclipsed structure and an angle of 36° indicates a staggered structure. Singlet, triplet, and quintet electronic states are designated by **S**, **T**, and **Q**, respectively.

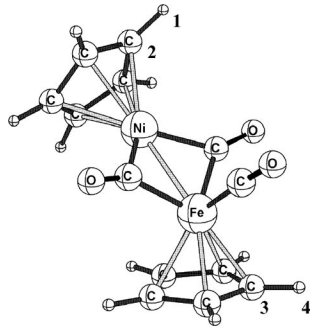

3-1

Figure 1. The structure of $Cp_2FeNi(CO)_3$ found in this work.

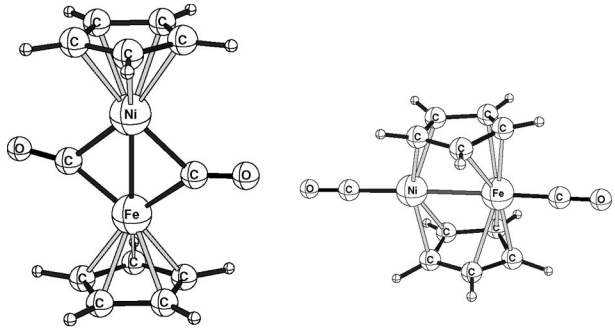

2-1 **2-2**

Figure 2. The two geometrical structures of $Cp_2FeNi(CO)_2$ found in this work.

3.1 Structures and Energetics

3.1.1 $Cp_2FeNi(CO)_3$

The coaxial structure **3**–**1** with two bridging CO groups and one terminal CO group bonded to the iron atom is found to be the global minimum for $Cp_2FeNi(CO)_3$ (Figure 1 and Table 1). The Fe–Ni distance in **3**–**1** of 2.46 Å is consistent with a single bond. No experimental crystal structure on the known $Cp_2FeNi(CO)_3$ is available for comparison with these theoretical results. However, this calculated Fe–Ni distance for **3**–**1** is consistent with the Fe–Ni distances in the range 2.43 to 2.56 Å found[43] by X-ray crystallography in the $NiFe_3C_2$ octahedron of $CpNiFe_3(CO)_7(\mu\text{-}PPh_2)(\mu_4,\eta^2\text{-}HC{\equiv}C\textit{i}Pr)$. Thus the FeNi bond in **3**–**1** may be considered to be a formal single bond.

The theoretical infrared active ν(CO) frequencies for structure **3**–**1S** at 1815 and 1984 cm^{-1} agree well with the experimental[44] values of 1816 and 1998 cm^{-1} and corre-

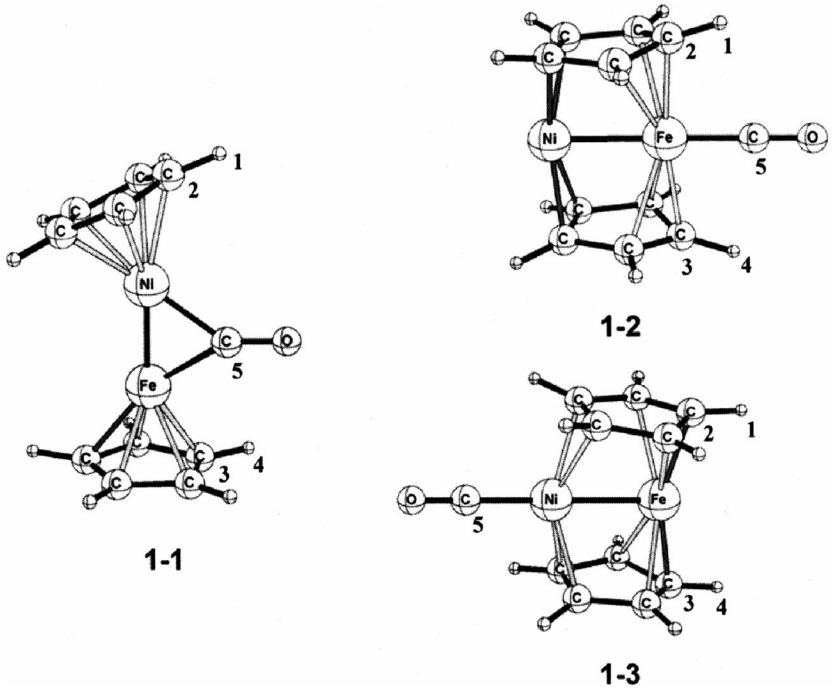

Figure 3. The three structures of $Cp_2FeNi(CO)$ found in this work. The numbers on atoms relate to the definitions of bond angles θ and dihedral angle τ in Table 3.

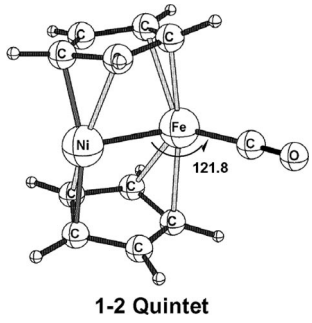

Figure 4. The anomalous structure of the quintet state **1**–**2Q** with a bent Ni–Fe–CO unit found in this work.

Table 1. Bond lengths [Å], dihedral angles $\tau_{(H1–C2–C3–H4)}$ [°], relative energies ΔE [in kcal/mol], approximate $<S^2>$ values, and ν(CO) frequencies [cm^{-1}] for the $Cp_2FeNi(CO)_3$ isomers at the BP86/DZP level of theory. Infrared intensities in parentheses are in km/mol.

	3–1S	**3–1T**
Symmetry	C_1	C_1
Fe–Ni	2.455	2.459
Fe–CO (bridge)	1.911	1.850
	1.911	1.850
Fe–CO (non-bridge)	1.755	1.850
	1.877	1.950
Ni–CO	1.877	1.950
$\tau_{(H1–C2–C3–H4)}$	32.2	–3.1
ΔE	0.0	26.3
$<S^2>$	0.00	2.04
ν(C–O)	1815 (842)	1813 (866)
	1845 (10)	1835 (10)
	1984 (780)	1965 (809)
Imaginary frequency	none	none

Table 2. Bond lengths [Å], relative energies ΔE [in kcal/mol], approximate $<S^2>$ values, and ν(CO) frequencies [cm^{-1}] for the $Cp_2FeNi(CO)_2$ isomers at the BP86/DZP level of theory. Infrared intensities in parentheses are in km/mol.

	2–1S	**2–1T**	**2–2S**	**2–2T**
Symmetry	C_s	C_1	C_s	C_s
Fe–Ni	2.353	2.389	2.475	2.555
Fe–CO	1.831	1.847	1.732	1.748
(bridge)	1.830	1.848		
Ni–CO	1.948	1.926	1.805	1.783
(bridge)	1.943	1.927		
ΔE	0.0	5.5	27.0	38.8
$<S^2>$	0.00	2.05	0.00	2.06
ν(CO)	1811 (944)	1803 (911)	1921 (1062)	1928 (1149)
	1836 (18)	1838 (9)	1979 (874)	1982 (784)
Imag. frequencies	none	none	none	none

spond to the antisymmetrical stretching mode of the two bridging CO groups and the stretching mode of the terminal CO group, respectively. The symmetrical stretching mode of the two bridging CO groups is predicted at 1845 cm^{-1}, with an infrared intensity too weak to be observed.

Structures of $Cp_2FeNi(CO)_3$ were also investigated in which the Fe–Ni bond is parallel to the Cp rings so that each metal atom is bonded to both Cp rings. However, such structures were found to lie more than 35 kcal/mol above **3**–**1** (see electronic supporting information).

3.1.2 $Cp_2FeNi(CO)_2$

Two optimized structures (**2**–**1** and **2**–**2** in Figure 2) are predicted for $Cp_2FeNi(CO)_2$. Structure **2**–**1** is a coaxial structure, $Cp_2FeNi(\mu\text{-}CO)_2$, with terminal η^5-Cp rings and

Table 3. Bond lengths [Å], bond angles $\theta_{(Fe–C5–O)}$ [°], dihedral angles $\tau_{(H1–C2–C3–H4)}$, relative energies ΔE [kcal/mol], approximate $<S^2>$ values, and ν(CO) frequencies [cm^{-1}] for the $Cp_2FeNi(CO)$ isomers at the BP86/DZP level of theory. Infrared intensities in parentheses are in km/mol.

Symmetry	**1–1S** C_1	**1–1T** C_1	**1–1Q** C_1	**1–2S** C_s	**1–2T** C_1	**1–2Q** C_1	**1–3S** C_1	**1–3T** C_1	**1–3Q** C_1
Fe–Ni	2.123	2.217	2.267	2.323	2.364	2.310	2.325	2.464	2.473
Fe–CO	1.868	1.917	2.104	1.731	1.744	1.850			
Ni–CO	1.923	1.858	1.764				1.805	1.800	1.773
$\theta_{(Fe–C5–O)}$	150.4	145.7	131.2	179.2	179.4	172.0	179.6	179.2	175.6
$\tau_{(H1–C2–C3–H4)}$	32.6	16.6	11.9	0.0	36.1	–23.1	0.0	0.0	–15.7
ΔE	4.6	4.1	2.1	0.0	11.3	26.8	25.1	11.9	15.2
$<S^2>$	0.00	2.26	6.04	0.00	2.05	6.07	0.00	2.05	6.03
ν(CO)	1856	1829	1867	1918	1920	1921	1975	1963	1965
	(561)	(590)	(602)	(855)	(891)	(1115)	(1014)	(1101)	(1211)
Imag. frequency	none	2*i*	none	none	none	none	none	none	none

two bridging CO ligands. Structure **2**–**2** is a perpendicular structure with two bridging Cp rings and two terminal CO ligands, namely $(\mu\text{-}Cp)_2FeNi(CO)$. This structure resembles a "hot dog" in which the "buns" are the Cp rings and the OCNiFeCO chain is the "meat." The Fe–Ni distances are longer in the triplet structures of $Cp_2FeNi(CO)_2$ than in the singlet isomers. The Fe–CO distances are generally smaller than the Ni–CO distances in all structures. This is consistent with the previous observation of shorter Fe–CO distances in $Fe(CO)_5$, namely 1.807 Å (axial) and 1.827 Å (equatorial),[45] than in $Ni(CO)_4$, namely 1.838 Å.[46] The energies of the "hot dog" singlet and triplet structures **2**–**2** are significantly higher than those of structure **2**–**1** (27.0 and 38.8 kcal/mol for singlet and triplet states, respectively). The global minimum for $Cp_2FeNi(CO)_2$ was found to be the singlet structure **2**–**1S**. The triplet structure **2**–**1T** is predicted to lie 5.5 kcal/mol higher than **2**–**1S**.

3.1.3 $Cp_2FeNi(CO)$

Three possible structures for $Cp_2FeNi(CO)$ (Figure 3) have been found. Structure **1**–**1** is a coaxial dimetallocene $Cp_2FeNi(\mu\text{-}CO)$ with a bridging CO group. The other two structures **1**–**2** and **1**–**3** have the metal–metal bond axis approximately perpendicular to the Cp ring axes (Figure 3) forming a "hot dog" shape perpendicular structure $(\mu\text{-}Cp)_2FeNi(CO)$ with bridging Cp ligands and a terminal CO group. The triplet and quintet electronic states of each structure have also been investigated, because the monocarbonyl complex represents a highly unsaturated molecular structure. Structure **1-2S** has C_s symmetry with the CO group bonded to iron, while structure **1**–**3S** has no symmetry with the CO group bonded to nickel. The energetic trend for each structure is quite different with respect to the singlet, triplet, and quintet electronic states. Thus for structure **1**–**1**, the quintet state has the lowest total energy. However, the singlet and triplet states are of the lowest energy for the two perpendicular structures **1**–**2** and **1**–**3**, respectively. The global minimum for all $Cp_2FeNi(CO)$ species is the singlet perpendicular structure **1**–**2S** with the CO group terminally bonded to the iron atom.

The Ni–Fe bond lengths in the $Cp_2FeNi(CO)$ isomers are predicted to be longer in the high spin states than in the singlet states except for **1**–**2**. For example, the Fe–Ni distances in **1**–**1** follow a trend **1**–**1Q** (2.267 Å) > **1**–**1T** (2.217 Å) > **1**–**1S** (2.123 Å). The same trend is found for isomer **1**–**3**, but not for **1**–**2** (Table 3). The orientation of the two Cp rings is quite different in the different electronic states for geometry **1**–**1**. In **1**–**1S**, the two rings are nearly staggered [$\tau_{(H1–C2–C3–H4)}$ is 32.6°]. However, in **1**–**1T** and **1**–**1Q**, the two rings prefer only partially staggered conformations [$\tau_{(H1–C2–C3–H4)}$ is 16.6° and 11.9°, respectively]. A very small imaginary frequency of 2*i* for **1**–**1T** arises from numerical integration errors.

In the perpendicular "hot dog" structures **1**–**2** and **1**–**3**, the Ni–Fe distances are significantly longer then those in the coaxial structure **1**–**1** for both the singlet and triplet isomers. Moreover, the terminal CO group binds more tightly to iron than to nickel as reflected implicitly by the shorter Fe–CO distance in **1**–**2** than the Ni–CO distance in **1**–**3** in both the singlet and triplet states. A similar trend is noted in comparing the first metal carbonyl dissociation energies of 41 ± 1 kcal/mol[47,48] in $Fe(CO)_5$ vs. 25 ± 2 kcal/mol[49] in $Ni(CO)_4$.

The **1**–**2Q** quintet state structure is special (Figure 4) with a non-linear Ni–Fe–CO unit (121.8°) in contrast to **1**–**2S** and **1**–**2T** with linear Ni–Fe–CO units. Structure **1**–**2Q** is also anomalous by having a predicted Ni–Fe distance shorter rather than that in the corresponding singlet **1**–**2S**.

3.2 Dissociation Energies

The CO dissociation energies for the $Cp_2FeNi(CO)_n$ complexes are listed in Table 4 based on the global minima and with the $Cp_2FeNi(CO)_{n-1}$ product in the same spin state as the reactant $Cp_2FeNi(CO)_n$. The positive CO dissociation energies indicate these reactions to be endothermic. Furthermore, the triplet isomers are found to have lower CO dissociation energies than the corresponding singlet isomers.

Table 4. Dissociation energies [kcal/mol] for the successive removal of carbonyl groups from $Cp_2FeNi(CO)_3$.

	B3LYP	BP86
$Cp_2FeNi(CO)_3$ (**3**–**1S**) → $Cp_2FeNi(CO)_2$ (**2**–**1S**) + CO	34.8	40.6
$Cp_2FeNi(CO)_3$ (**3**–**1T**) → $Cp_2FeNi(CO)_2$ (**2**–**1T**) + CO	9.5	19.8
$Cp_2FeNi(CO)_2$ (**2**–**1S**) → $Cp_2FeNi(CO)$ (**1**–**1S**) + CO	49.5	65.3
$Cp_2FeNi(CO)_2$ (**2**–**1T**) → $Cp_2FeNi(CO)$ (**1**–**1T**) + CO	36.2	59.3

3.3 Comparison Between $Cp_2FeNi(CO)_n$ and $Cp_2Co_2(CO)_n$

3.3.1 $Cp_2FeNi(CO)_3$ vs. $Cp_2Co_2(CO)_3$

The asymmetry of the dimetal unit in $Cp_2FeNi(CO)_3$ leads to a different structure than that found for the isoelectronic $Cp_2Co_2(CO)_3$ in order for both metal atoms to have the favored 18-electron configurations with a formal metal–metal single bond (Figure 5). Thus for $Cp_2Co_2(CO)_3$ the experimentally known structure[16] is $Cp_2Co_2(CO)_2(\mu\text{-}CO)$ with a single bridging CO group. However, an alternative structure $Cp_2Co_2(\mu\text{-}CO)_3$ with three bridging CO groups is predicted[17] to have a similar energy. For the isoelectronic $Cp_2FeNi(CO)_3$ the global minimum is $Cp_2Fe(CO)Ni(\mu\text{-}CO)_2$ with two bridging CO groups rather than one or three bridging CO groups. The third CO group in this $Cp_2Fe(CO)Ni(\mu\text{-}CO)_2$ structure is a terminal CO group bonded to the iron atom, so that both the iron and nickel atoms have equivalent electronic configurations, namely the favored 18-electron configuration. Thus the asymmetry of the metal–metal bond in $Cp_2FeNi(CO)_3$ relative to $Cp_2Co_2(CO)_3$ leads to a redistribution of the metal carbonyl groups.

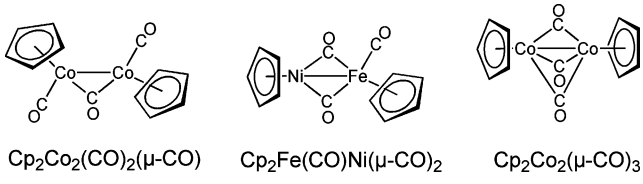

Figure 5. Alternative structures for $Cp_2MM'(CO)_3$ derivatives.

The metal–metal bond lengths in $Cp_2MM'(CO)_3$ derivatives decrease monotonically as the number of bridging CO groups increases in the series $Cp_2Co_2(CO)_2(\mu\text{-}CO) > Cp_2Fe(CO)Ni(\mu\text{-}CO)_2 > Cp_2Co_2(\mu\text{-}CO)_3$ irrespective of whether the dimetal unit is Co_2 or FeNi with BP86 values of 2.506 Å, 2.455 Å, and 2.352 Å, respectively. The available information does not provide information as to whether the metal–metal interactions in these binuclear compounds are direct interactions or occur through the carbonyl bridges. Even for the less complicated homoleptic analogue $Fe_2(CO)_9$, detailed studies[50] do not provide clear and definitive insight into this question.

3.3.2 $Cp_2FeNi(CO)_2$ vs. $Cp_2Co_2(CO)_2$

The global minima for the isoelectronic dicarbonyl compounds $Cp_2Co_2(\mu\text{-}CO)_2$ and $Cp_2FeNi(\mu\text{-}CO)_2$ are coaxial structures with the same arrangements of their two CO groups, namely as two bridging groups. The metal–metal distances [2.346 Å for $Cp_2Co_2(\mu\text{-}CO)_2$ and 2.353 Å for $Cp_2FeNi(\mu\text{-}CO)_2$] are essentially identical and enough less than the 2.455 Å Fe–Ni doubly bridged single bond length in $Cp_2Fe(CO)Ni(\mu\text{-}CO)_2$ to be regarded as the M=M double bonds needed to give both metal atoms the favored 18-electron configurations. The perpendicular "hot dog" isomers $(\mu\text{-}Cp)_2M_2(CO)_2$ (M_2 = Co_2 or FeNi) have essentially similar structures with metal–metal distances (BP86) of 2.427 Å for $(\mu\text{-}Cp)_2Co_2(CO)_2$ and 2.468 Å for $(\mu\text{-}Cp)_2FeNi_2(CO)_2$.

3.3.3 $Cp_2FeNi(CO)$ vs. $Cp_2Co_2(CO)$

The isoelectronic species $Cp_2Co_2(CO)$ was reinvestigated[32] for comparison with $Cp_2FeNi(CO)$ using the same level of theory. The singlet states of $Cp_2Co_2(CO)$ were studied in the previous work using a coarser integration grid (75,302) than the (99,590) integration grid used in this work; this leads to some significant imaginary frequencies.[17] Our new results on $Cp_2Co_2(CO)$ including not only recomputed singlet electronic states but also the first investigations of triplet and quintet electronic states are listed at Table 5 and Figure 6. The energetic trend of different electronic states for both the coaxial dimetallocene $Cp_2Co_2(\mu\text{-}CO)$ **Co-1** and the perpendicular dimetallocene $(\mu\text{-}Cp)_2Co_2(CO)$ **Co-2** is consistent with singlet < triplet < quintet. The isomer **Co-1S** is again found to be a

Table 5. Bond lengths [Å], approximate $<S^2>$ values, and ν(CO) frequencies [cm^{-1}] for the $Cp_2Co_2(CO)$ isomers at the BP86/DZP level of theory. Infrared intensities in parentheses are in km/mol.

	Co-1S	**Co-1T**	**Co-1Q**	**Co-2S**	**Co-2T**	**Co-2Q**
Symmetry	C_{2v}	C_1	C_1	C_s	C_1	C_1
Co–Co	2.050	2.144	2.242	2.295	2.384	2.355
Co–CO	1.905	1.831	1.921	1.741	1.737	1.776
	1.905	1.953	1.868			
ΔE	0.0	7.3	9.6	6.3	20.0	28.3
$<S^2>$	0.00	2.06	6.04	0.00	2.04	6.05
ν(CO)	1870 (583)	1840 (593)	1837 (574)	1939 (933)	1936 (1000)	1932 (1241)
Imaginary frequency	no	no	no	no	no	no

global minimum. The metal–metal distances are longer in the perpendicular structure than those in the coaxial structure of the homometallic $Cp_2Co_2(CO)$, as found here for the heterometallic $Cp_2FeNi(CO)$.

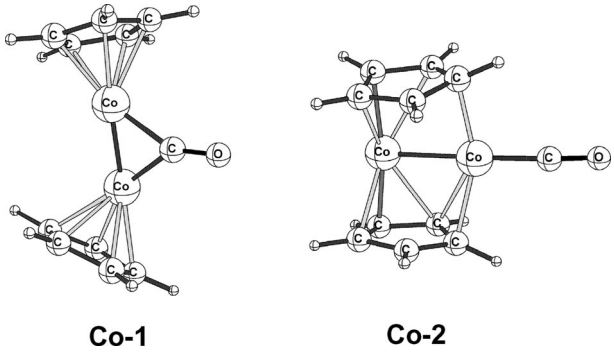

Figure 6. The two structures of $Cp_2Co_2(CO)$ with high-spin states (triplet and quintet) investigated in this work.

Plots of the spin densities of all open-shell species of the $Cp_2FeNi(CO)$ and $Cp_2Co_2(CO)$ isomers are displayed in Figure 7. In the $Cp_2FeNi(CO)$ triplet states, the spin densities are almost exclusively concentrated on the iron atom, consistent with a 16-electron configuration for the iron atom and an 18-electron configuration for the nickel atom. Even in the quintet states, the spin density is still concentrated largely on iron. However, in the homometallic binuclear $Cp_2Co_2(CO)$ structures, the unpaired electron density is evenly distributed on each cobalt atom. None of the triplet or quintet isomers of $Cp_2FeNi(CO)_n$ (n = 3, 2, 1) or $Cp_2Co_2(CO)$ exhibits any significant spin contamination as indicated by approximate $<S^2>$ values close to the ideal values of 2 and 6 for the triplets and quintets, respectively.

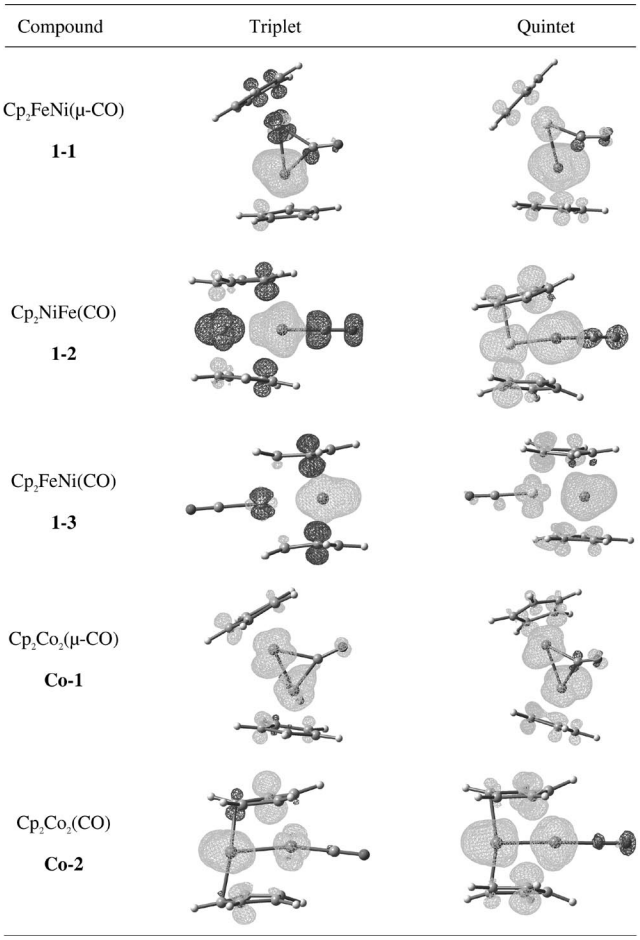

Figure 7. The spin densities of triplet and quintet states of $Cp_2Co_2(CO)$ and isoelectronic species $Cp_2FeNi(CO)$ at the BP86/DZP level. Positive and negative values are represented by gray and black mesh cloud, respectively.

The isoelectronic pair of monocarbonyl compounds $Cp_2Co_2(CO)$ and $Cp_2FeNi(CO)$ have qualitatively similar structures. The CO group in the coaxial isomers (e.g., **1**–**1**) bridges the metal–metal bond, which is short enough by BP86 [2.050 Å for $Cp_2Co(\mu\text{-}CO)$ and 2.123 Å for $Cp_2FeNi(\mu\text{-}CO)$] to be considered to be the triple bond required to give both metal atoms the favored 18-electron configurations for the singlet state. Compared to the energetic trend of singlet < triplet < quintet for the $Cp_2Co_2(\mu\text{-}CO)$ coaxial isomer (**Co-1**), a reversed energetic trend is found for the $Cp_2FeNi(\mu\text{-}CO)$ coaxial isomer (**1**–**1**), in which a quintet state has relatively the lowest energy. This indicates that for heterometallic complexes, a high spin state with unbalanced density distribution between two metals (Figure 7) might be favored instead of a multiple metal–metal bond. The isoelectronic set of three perpendicular complexes $Cp_2Co_2(CO)$, $Cp_2Fe(CO)Ni$ (**1**–**2** in Figure 3) and $Cp_2FeNi(CO)$ (**1**–**3** in Figure 3) all have essentially the same structures with metal–metal distances in the narrow range 2.29–2.33 Å.

4. Conclusion

A coaxial structure $Cp_2Fe(CO)Ni(\mu\text{-}CO)_2$ with two bridging carbonyl compounds and one terminal carbonyl has been found to be the global minimum for the tricarbonyl $Cp_2FeNi(CO)_3$. Compared with $Cp_2FeNi(CO)_3$, the isoelectronic $Cp_2Co_2(CO)_3$ has two coaxial minima with different structures, namely $Cp_2Co_2(CO)_2(\mu\text{-}CO)$ with a single bridging carbonyl and $Cp_2Co_2(\mu\text{-}CO)_3$ with all three carbonyl groups in bridging positions. The isoelectronic pair of dicarbonyl compounds $Cp_2FeNi(CO)_2$ and $Cp_2Co_2(CO)_2$ have essentially the same structures for both coaxial and perpendicular isomers. The coaxial structure of the monocarbonyl $Cp_2FeNi(CO)$ prefers an open-shell high spin state whereas the isoelectronic $Cp_2Co_2(CO)$ prefers a closed shell state with a Co≡Co triple bond. However, the global minimum for the monocarbonyl is a singlet perpendicular $Cp_2FeNi(CO)$ structure with a terminal CO group bonded to the iron atom.

Supporting Information (see also the footnote on the first page of this article): Tables S1–S4: bond lengths [Å], bond angles $\theta_{(Fe\text{–}C5\text{–}O)}$ [°], dihedral angles $\tau_{(H1\text{–}C2\text{–}C3\text{–}H4)}$ [°], relative energies [kcal/mol] and ν(CO) frequencies [cm^{-1}] for various spin states of the $Cp_2FeNi(CO)_n$ (n = 3, 2, 1) and $Cp_2Co_2(CO)$ isomers at the B3LYP/DZP level of theory; Tables S5–S14: theoretical harmonic vibrational frequencies [cm^{-1}] and their infrared intensities [km/

mol] for various spin states of the $Cp_2FeNi(CO)_n$ (n = 3, 2, 1) and $Cp_2Co_2(CO)$ isomers.

Acknowledgments

We are grateful to the National Science Foundation (NSF) for support of this work under grants CHE-0209857, CHE-0451445, and CHE-0716718. J. D. Z. thanks Dr. Jiande Gu for help in preparing spin-density plots. We also thank the Research Computing Center of the University of Georgia for providing computational resources.

[1] R. B. King, M. B. Bisnette, *J. Organomet. Chem.* **1967**, *8*, 287–297.
[2] F. A. Cotton, L. Kruczynski, B. A. Frenz, *J. Organomet. Chem.* **1978**, *160*, 93–100.
[3] M. D. Curtis, W. M. Butler, *J. Organomet. Chem.* **1978**, *155*, 131–145.
[4] R. J. Klingler, W. M. Butler, M. D. Curtis, *J. Am. Chem. Soc.* **1978**, *100*, 5034–5039.
[5] I. Bernal, J. D. Korp, W. A. Herrmann, R. Serrano, *Chem. Ber.* **1984**, *117*, 434–444.
[6] J. K. Hoyano, W. A. G. Graham, *Organometallics* **1982**, *1*, 783–787.
[7] C. P. Casey, H. Sakaba, P. N. Hazin, D. R. Powell, *J. Am. Chem. Soc.* **1991**, *113*, 8165–8166.
[8] J. P. Blaha, B. E. Bursten, J. C. Dewan, R. B. Frankel, C. L. Randolph, B. A. Wilson, M. S. Wrighton, *J. Am. Chem. Soc.* **1985**, *107*, 4561–4562.
[9] W. I. Bailey Jr, D. M. Collins, F. A. Cotton, J. C. Baldwin, *J. Organomet. Chem.* **1979**, *165*, 373–381.
[10] M. Green, D. R. Hankey, J. A. K. Howard, P. Louca, F. G. A. Stone, *J. Chem. Soc. Chem. Commun.* **1983**, 757–758.
[11] T. Madach, H. Vahrenkamp, *Chem. Ber.* **1980**, *113*, 2675–2685.
[12] J. F. Tilney-Bassett, *Proc. Chem. Soc. London* **1960**, 419, CAN 55:54225 AN 1961:54225.
[13] J. F. Tilney-Bassett, *J. Chem. Soc.* **1963**, 4784–4788.
[14] K. Yasufuku, H. Yamazaki, *J. Organomet. Chem.* **1971**, *28*, 415–421.
[15] K. Yasufuku, H. Yamazaki, *J. Organomet. Chem.* **1972**, *38*, 367–372.
[16] F. R. Anderson, M. S. Wrighton, *Inorg. Chem.* **1986**, *25*, 112–114.
[17] H. Wang, Y. Xie, R. B. King, H. F. Schaefer, *J. Am. Chem. Soc.* **2005**, *127*, 11646–11651.
[18] K. P. C. Vollhardt, J. E. Bercaw, R. G. Bergmann, *J. Organomet. Chem.* **1975**, *97*, 283–297.
[19] E. R. Davidson (guest editor), *Chem. Rev.*, Special Issue on Computational Transition Metal Chemistry, February, **2000**.
[20] C. J. Barden, J. C. Rienstra-Kiracofe, H. F. Schaefer, *J. Chem. Phys.* **2000**, *113*, 690–700.
[21] B. N. Papas, H. F. Schaefer, *J. Chem. Phys.* **2005**, *123*, 074321/1–074321/12.
[22] A. W. Ehlers, G. Frenking, *J. Am. Chem. Soc.* **1994**, *116*, 1514–1520.
[23] B. Delley, M. Wrinn, H. P. Lüthi, *J. Chem. Phys.* **1994**, *100*, 5785–5791.
[24] J. Li, G. Schreckenbach, T. Ziegler, *J. Am. Chem. Soc.* **1995**, *117*, 486–494.
[25] V. Jonas, W. Thiel, *J. Chem. Phys.* **1995**, *102*, 8474–8484.
[26] T. A. Barckholtz, B. E. Bursten, *J. Am. Chem. Soc.* **1998**, *120*, 1926–1927.
[27] S. Niu, M. B. Hall, *Chem. Rev.* **2000**, *100*, 353–405.
[28] P. Macchi, A. Sironi, *Coord. Chem. Rev.* **2003**, *238*, 383–412.
[29] J.-L. Carreon, J. N. Harvey, *Phys. Chem. Chem. Phys.* **2006**, *8*, 93–100.
[30] M. Bühl, H. Kabrede, *J. Chem. Theory Comput.* **2006**, *2*, 1282–1290.
[31] See especially F. Furche, J. P. Perdew, *J. Chem. Phys.* **2006**, *124*, 044103/1–044103/27.
[32] X. Feng, J. Gu, Y. Xie, R. B. King, H. F. Schaefer, *J. Chem. Theory Comput.* **2007**, *3*, 1580–1587.
[33] H. Y. Wang, Y. Xie, R. B. King, H. F. Schaefer, *J. Am. Chem. Soc.* **2006**, *128*, 11376–11384.
[34] A. D. Becke, *Phys. Rev. A* **1988**, *38*, 3098–3100.
[35] J. P. Perdew, *Phys. Rev. Lett.* **1985**, *55*, 1665–1668.
[36] T. H. Dunning, *J. Chem. Phys.* **1970**, *53*, 2823–2833.
[37] S. Huzinaga, *J. Chem. Phys.* **1965**, *42*, 1293–1302.
[38] A. J. H. Wachters, *J. Chem. Phys.* **1970**, *52*, 1033–1036.
[39] D. M. Hood, R. M. Pitzer, H. F. Schaefer, *J. Chem. Phys.* **1979**, *71*, 705–712.
[40] a) M. J. Frisch, G. W. Trucks, H. B. Schlegel, P. M. W. Gill, B. G. Johnson, M. A. Robb, J. R. Cheeseman, T. A. Keith, G. A. Petersson, J. A. Montgomery, K. Raghavachari, M. A. Al-Laham, V. G. Zakrzewski, J. V. Ortiz, J. B. Foresman, J. Cioslowski, B. B. Stefanov, A. Nanayakkara, M. Challacombe, C. Y. Peng, P. Y. Ayala, W. Chen, M. W. Wong, J. L. Andres, E. S. Replogle, R. Gomperts, R. L. Martin, D. J. Fox, J. S. Binkley, D. J. Defrees, J. Baker, J. P. Stewart, M. Head-Gordon, C. Gonzalez, J. A. Pople, *Gaussian 94*, Gaussian, Inc., Pittsburgh, PA, **1995**; used by J. D. Zhang. b) M. J. Frisch, G. W. Trucks, H. B. Schlegel, G. E. Scuseria, M. A. Robb, J. R. Cheeseman, J. A. Montgomery, Jr., T. Vreven, K. N. Kudin, J. C. Burant, J. M. Millam, S. S. Iyengar, J. Tomasi, V. Barone, B. Mennucci, M. Cossi, G. Scalmani, N. Rega, G. A. Petersson, H. Nakatsuji, M. Hada, M. Ehara, K. Toyota, R. Fukuda, J. Hasegawa, M. Ishida, T. Nakajima, Y. Honda, O. Kitao, H. Nakai, M. Klene, X. Li, J. E. Knox, H. P. Hratchian, J. B. Cross, V. Bakken, C. Adamo, J. Jaramillo, R. Gomperts, R. E. Stratmann, O. Yazyev, A. J. Austin, R. Cammi, C. Pomelli, J. W. Ochterski, P. Y. Ayala, K. Morokuma, G. A. Voth, P. Salvador, J. J. Dannenberg, V. G. Zakrzewski, S. Dapprich, A. D. Daniels, M. C. Strain, O. Farkas, D. K. Malick, A. D. Rabuck, K. Raghavachari, J. B. Foresman, J. V. Ortiz, Q. Cui, A. G. Baboul, S. Clifford, J. Cioslowski, B. B. Stefanov, G. Liu, A. Liashenko, P. Piskorz, I. Komaromi, R. L. Martin, D. J. Fox, T. Keith, M. A. Al-Laham, C. Y. Peng, A. Nanayakkara, M. Challacombe, P. M. W. Gill, B. Johnson, W. Chen, M. W. Wong, C. Gonzalez, J. A. Pople, *Gaussian 03*, Gaussian, Inc., Wallingford CT, **2004**; used by Z. Chen.
[41] B. N. Papas, H. F. Schaefer, *J. Mol. Struct. theochem* **2006**, *768*, 175–181.
[42] Y. Xie, H. F. Schaefer, R. B. King, *J. Am. Chem. Soc.* **2000**, *122*, 8746–8761.
[43] E. Sappa, D. Belletti, A. Tiripicchio, M. Camellini, *J. Organomet. Chem.* **1989**, *359*, 419–428.
[44] P. McArdle, A. R. Manning, *J. Chem. Soc. A* **1971**, 717–719.
[45] H. P. Lüthi, P. E. M. Siegbahn, J. Almlöf, *J. Phys. Chem.* **1985**, *89*, 2156–2161.
[46] L. Hedberg, T. Iijima, K. Hedberg, *J. Chem. Phys.* **1979**, *70*, 3224–3229.
[47] K. E. Lewis, D. M. Golden, G. P. Smith, *J. Am. Chem. Soc.* **1984**, *106*, 3905–3912.
[48] R. Huq, A. J. Pöe, S. Chawla, *Inorg. Chim. Acta* **1980**, *38*, 121–125.
[49] A. E. Stevens, C. S. Feigerle, W. C. Lineberger, *J. Am. Chem. Soc.* **1982**, *104*, 5026–5031.
[50] A. Rosa, E. J. Baerends, *New J. Chem.* **1991**, *125*, 815–829.

Received: October 2, 2007
Published Online: January 24, 2008

